Computational Materials Science 138 (2017) 27–33

Contents lists available at ScienceDirect

Computational Materials Science

journal homepage: www.elsevier.com/locate/commatsci

Stress and damage development in the carbonization process of manufacturing carbon/carbon composites

Tiantian Yin, Yu Wang *, Linghui He, Xinglong Gong *

CAS Key Laboratory of Mechanical Behavior and Design of Materials, Department of Modern Mechanics, University of Science and Technology of China, Hefei 230027, China

ARTICLE INFO

Article history:
Received 4 May 2017
Received in revised form 12 June 2017
Accepted 13 June 2017

Keywords:
Carbonization process
Chemical shrinkage
Carbon/carbon composites
Damage evolution

ABSTRACT

Carbon/carbon composites are widely used in aerospace industry due to their excellent mechanical and thermal properties in high temperature. However, understanding of the mechanism for defects induced in the carbonization process of carbon/carbon composites is still inadequate. In this paper, a model is established to obtain the matrix properties and simulate the stress and damage evolution during the carbonization process of carbon/carbon composites. First, the phase evolution equations are used to gain the volume fractions of phases, and then the elastic modulus and Poisson ratio are obtained by a nested homogenization method. Then, the thermal deformation including the competition between thermal expansion and chemical shrinkage is discussed. The damage evolution in the matrix is incorporated through the progressive damage model. Finally, we perform the finite element simulation for the carbonization of the unidirectional fiber bundle reinforced carbon/carbon composites. The results show that matrix sustains compression circumferential stress before reaction start. After reaction activates, the circumferential stress turns to tension due to the matrix shrinkage, and the tension stress increases rapidly to cause damage. The damage evolves along the fiber/matrix interface with the temperature increasing. With damage accumulation, micro cracks may generate along the fiber/matrix interface, which is similar as the literature reported.

© 2017 Elsevier B.V. All rights reserved.

1. Introduction

Carbon/carbon composites possess many excellent properties over other conventional materials, such as high ratio of mechanical properties versus density at high temperature, low thermal expansion, and high thermal and chemical stability [1–3]. As an attractive material in aerospace field, the demands for this material have increased tremendously recently. In order to obtain satisfactory products, a fundamental understanding of the manufacture process is essential for quality control and product optimization.

The preparation of carbon/carbon composite materials can be roughly divided into three steps: The resin is firstly impregnated into the carbon fiber architectures. After that, the composite is put into the furnace for carbonization in a flow of nitrogen. Finally, the densification process is adopted until reaching the desired density. In the carbonization process, the pyrolysis reactions convert the resin matrix to amorphous carbon phase and gas phase. Gaseous products are released and a highly porous carbon/carbon preform are left. The actual process of thermodecomposition in the manufacture of carbon/carbon composites materials is very complex, which involves many coupled mechanisms, both mechanically and chemically. Various events such as phases tranformation, internal stress and strain generation, internal damage and defects, and matrix degradation exist simultaneously at the same process, and they have large effects on each other. The detailed physical and mechanical essence are still not clearly described.

A large number of researches have been carried out on the carbonization process of carbon/carbon composites. However, most of these researches foucs on the chemical reaction kinetics [4–6]. Only a few studies concern about the evolutions of stress and damage during the carbonization. Dimitrienko [7–11] proposed a porous materials model to obtain the volume fraction of resin, carbon and gas during the carbonization process and then the effective mechanical properties, thermal deformation considering the chemical shrinkage and stress characteristics were discussed. Schulte-Fischedick [12–15] identified different crack types that occured during carbonization process using thermo-microscopy and acoustic emission analysis. They noted that the creation of cracks were driven by the high shrinkage of matrix. Kim [16–19] established a model for stress and displacement predictions using two-dimensional finite element method. In his model, the composites properties were gained by the micro-mechanical model pro-

* Corresponding authors.
E-mail addresses: wyu@ustc.edu.cn (Y. Wang), gongxl@ustc.edu.cn (X. Gong).

http://dx.doi.org/10.1016/j.commatsci.2017.06.014
0927-0256/© 2017 Elsevier B.V. All rights reserved.

posed by Bogetti [20] and the mechanical property degradation was simulated based on the crack density from the experiment. Besides, Rajneesh Sharma [21–23] found that there exsited voids and cracks in manufactured carbon/carbon composites which were induced during manufacturing process, and they furtherly proved that the internal defects had a larger effect of on the mechanical properties of carbon/carbon composite materials.

So far, the mechanism of the internal stress generation and the formation of local defects are still not accurately described. The competition between thermal deformation and chemical shrinkage and its effects on the internal stress still need to be discussed. The aim of this paper is to investigate the mechanism for internal stress generation and damage developments during the carbonization process by numerical methods. First of all, a basic model to describe the evolution of volumetric fraction for different phases is introduced. And then, the thermal deformation behaviors including the competition between thermal expansion and chemical shrinkage are discussed, which will be taken into the final meso-mechanical finite element (FE) model. A progressive damage model is also adopted into the FE model for simulating the internal damage evolution in matrix. Finally, a FE analysis on a representative unit cell for unidirectional fiber bundle reinforced carbon/carbon composites is performed to study the internal stress generation, the internal damage formation and evolution during carbonization process.

2. Related equations in the carbonization process

2.1. The phase evolution equations and the effective elastic properties

During the carbonization process, the resin matrix is transformed into pyrolytic carbon and gas. Therefore, chemical compositions of the composite changes with the temperature. Besides the reinforcing fiber, there are four phases in the matrix: solid resin, liquid resin, pyrolytic carbon and gas. Because the liquid resin only exists in the initial stage of carbonization and its amount is pretty small comparing to solid resin, it is ignored in the next phase evolution equations. And since most generated gas is released, the gas phase is replaced by void phase in the subsequent discussion. When the pyrolysis of the matrix happens, the volume fraction of the three phases vary and satisfy the following relationship: $\phi_r + \phi_c + \phi_v = 1$, where ϕ_r, ϕ_c and ϕ_v are the volume fraction of resin phase, pyrolytic carbon phase and voids phase, respectively. Eventually, the volume fraction evolution equations of each phase in the carbonization process are described as follows, which are based on heat-mass transfer relationship [7].

$$\begin{cases} \rho_r \frac{\partial \phi_r}{\partial t} = -J_r \\ \rho_c \frac{\partial \phi_c}{\partial t} = (1-\Gamma_r) J_r \end{cases} \tag{1}$$

where ρ_r, ρ_c are densities of solid resin phase and pyrolytic carbon phase, respectively. Γ_r is the gasification coefficient concerning to the phase transformation. The rate of the pyrolysis reaction J_r is described by the equation in the Arrhenius type:

$$J_r = J_r^0 \phi_r \exp\left(-\frac{Ea_r}{RT}\right) \tag{2}$$

here T is current temperature, J_r^0 and Ea_r are pre-exponential factor and activation energy of the thermal pyrolysis reaction of the matrix. Based on above equations, the phase fraction evolution in the composite can be determined with the temperature variation of the system.

Due to transformations of compositions, the material properties of matrix are changing in the carbonization process. As the composites are made of three different phases at the same time, a nested homogenization method based on the Mori-Tanaka model is used to estimate the effective elastic properties. In the first step, the solid resin as a matrix is homogenized with the pyrolytic carbon as the inclusion. And then the effective material whose properties are obtained above acts as a fictitious matrix reinforced with voids as another inclusion to constitute the real material. The trial computation shows that the sequence of the inclusion has few influence on the final results.

2.2. The thermal deformation behaviors of matrix

In conventional fiber reinforced polymer matrix composites, one important reason for the residual stresses/strains generation is the mismatch in the coefficient of thermal expansion (CTE) of the fiber and matrix. As for carbon/carbon composites during carbonization process, things get more complicated. The thermal deformation of matrix is not just depended on the thermal expansion. The chemical shrinkage induced by the pyrolysis reaction would also change the volume of matrix. With the phase transformation, the competition between thermal expansion and chemical shrinkage will change, and thus affect the thermal deformation of matrix.

Thus, during the carbonization process, the thermal deformation of matrix identified by the thermal strain ε_m, can be divided into three parts: the thermal expansion of resin matrix, the thermal expansion of carbon matrix and the chemical shrinkage due to reaction. It can be expressed as [7]:

$$\varepsilon_m = \alpha_r \phi_r (T - T_0) + \alpha_c \int_0^t \dot{\phi}_c (T(t) - T(\tau)) d\tau - \beta_c \phi_c \tag{3}$$

here α_r and α_c are the thermal expansion coefficients of resin matrix and carbon matrix, respectively. β_c is the chemical shrinkage coefficient. T_0 is the reference temperature.

Finally, the apparent thermal expansion coefficient α_{eff} during the carbonization process can be defined as:

$$\alpha_{eff} = \varepsilon_m / (T - T_0) \tag{4}$$

When α_{eff} is positive, it means the matrix expand with temperature increasing. Otherwise, the matrix shrinkage happens.

2.3. Evolution of damage

A progressive damage model is introduced to simulate the initialization and evolution of damage in matrix during carbonization process. The material behavior is assumed to be isotropic. When the maximum principal strain ε_{max} exceeds the failure strain ε_d, the material begins to be damaged and the damage factor evolves according to the equation as follow:

$$d = 1 - \frac{\varepsilon_d}{\varepsilon_{\max}} \exp\left(-\frac{C_0 \varepsilon_d (\varepsilon_{\max} - \varepsilon_d) L_c}{G_m}\right) \tag{5}$$

where C_0 is the initial stiffness of the matrix without any damage, and L_c is the characteristic length associated with the elements geometry, which does help to minimize the mesh sensitivity in the numerical simulation [24]. G_m is a parameter which control the failure progresses.

The initiation and evolution of the damage would induce the materials degradation. Thus, the local effective elastic properties is updated once the damage increases, and then the local stress status need to be re-calculated to check whether new damage happens before next iteration.

3. Numerical model

The meso-mechanical model is set up based on the representative volume element (RVE) technique. A 2D unit cell of a unidirec-

tional fiber reinforced carbon/carbon composite is shown in Fig. 1 (a). The fiber bundle locates in the middle of the unit cell surrounding by matrix. The fiber volume fraction is 50%. The thermal expansion coefficient of the carbon fiber is 13 ppm/°C [14]. The fiber bundle/matrix interface is perfectly bonded. It is assumed that no any reaction inside the carbon fiber, which means the mechanical properties do not change during the carbonization process. The matrix is made of three different phases at the same time, as Fig. 1(b) shows. The phase transformation, mechanical properties variation, thermal deformation evolution and also damage generation in the matrix are integrated into a constitutive model by using the UMAT program of ABAQUS. The parameters of the matrix used in this model are listed in Table 1. The values of them are based on experiments and literatures [7,25,26].

The periodic boundary conditions are imposed along the outer boundary of RVE. The temperature gradient inside the RVE caused by heat conduction is ignored. And the temperature inside the RVE is uniformly heated from room temperature (RT) up to 1000 °C with rate of 5 °C/min. Therefore, the internal stress/strain and damage evolution of the unit cell during the carbonization process are analyzed by ABAQUS.

4. Results and discussions

4.1. The matrix properties during carbonization

The volume fractions of solid resin, carbon and voids vary with temperature as Fig. 2 illustrated. The transformation of different compositions due to the pyrolysis reaction mainly take place in the temperature interval between 300 °C and 800 °C. As from Fig. 2, the volume fraction of resin reduces from 100% to zero, while at the same time, the volume fraction of carbon and voids increase from 0 to 58% and 42% respectively. The variation of compositions would have an impact on the mechanical properties of the matrix. It can be seen in Fig. 3, the effective elastic modulus and Poisson ratio also vary with the reaction progress. At the initial stage of the pyrolysis reaction, the effective elastic modulus is declined due to the appearance of voids. And then with the volume fraction of pyrolytic carbon increasing, the influence of carbon with higher elastic properties would dominate the evolution of the mechanical properties of matrix. As a result, the effective elastic modulus turns to increase from 550 °C. Finally, the effective elastic modulus reaches about 4.11 GPa when the reaction finished.

The thermal strain and the apparent thermal expansion coefficient are plotted in Fig. 4. Below 300 °C, the thermal strain of the matrix mainly depends on the thermal expansion of resin since the pyrolysis reaction has not happened yet. And the apparent thermal expansion coefficient keeps constant. With the pyrolysis reaction activates, the negative thermal strain is major caused by the chemical shrinkage. And thus the apparent thermal expansion coefficient of matrix is reduced with the temperature increasing. At the final stage, due to the end of the reaction, the thermal strain of matrix only comes from the thermal expansion of carbon. According to Eq. (4), the apparent thermal expansion coefficient is chosen as a secant value. Thus the absolute value of the coefficient α_{eff} reduces at the final stage due to the increasing of the temperature difference.

Table 1
The material parameters of matrix in carbonization model.

Parameter	Value	Parameter	Value
J_r^0	2180 kg s/m^3	E_r	3.5 GPa
Ea_r	6800 K	E_c	10 GPa
Γ_r	0.1	μ_r	0.41
ρ_c	1700 kg/m^3	μ_c	0.35
ρ_r	1100 kg/m^3	α_r	50 (ppm/°C)
ε_d	0.0285	α_c	6 (ppm/°C)
G_m	1000 (N/m)	β_c	0.36

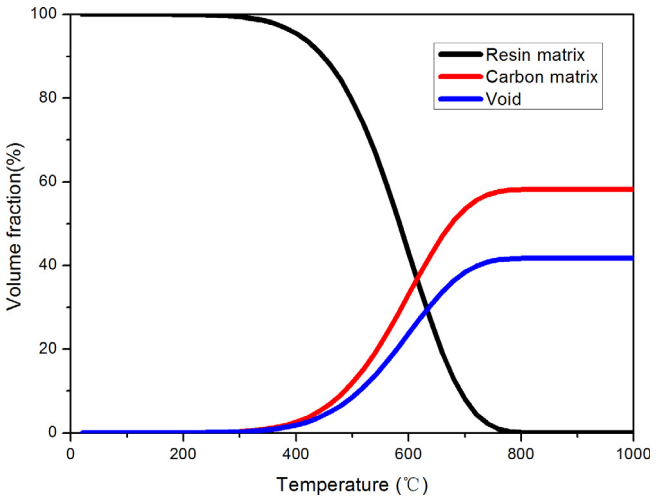

Fig. 2. The volume fraction of each phase.

4.2. Stress and damage developments

The stress and damage developments of the RVE are calculated during carbonization process. The circumferential stress $\sigma_{\theta\theta}$ in local cylindrical coordinates system is shown in Fig. 5 and the cor-

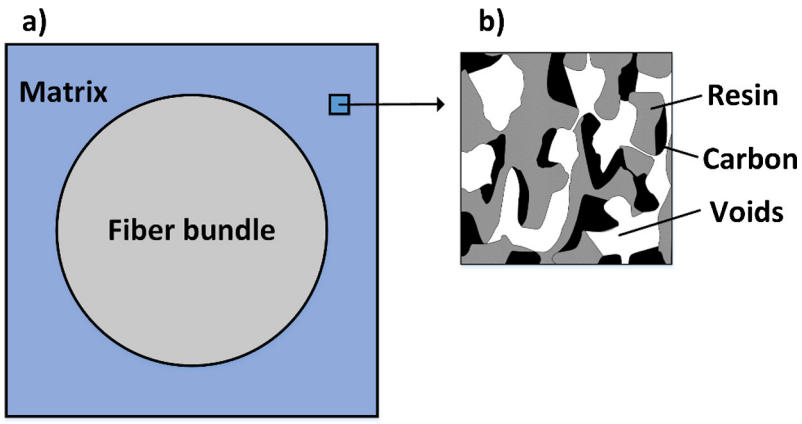

Fig. 1. (a) RVE of unidirectional fiber reinforced composites. (b) Infinitesimal volume of the matrix.

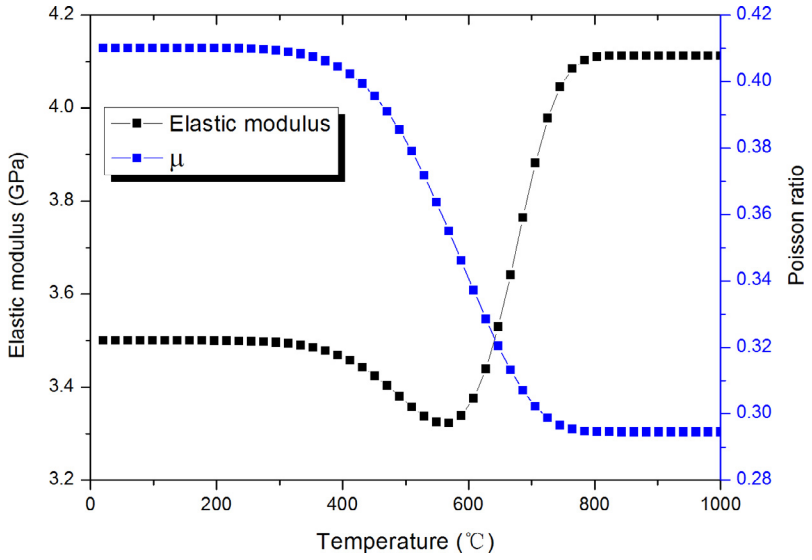

Fig. 3. The effective elastic modulus and Poisson ratio calculated via the nested homogenization method.

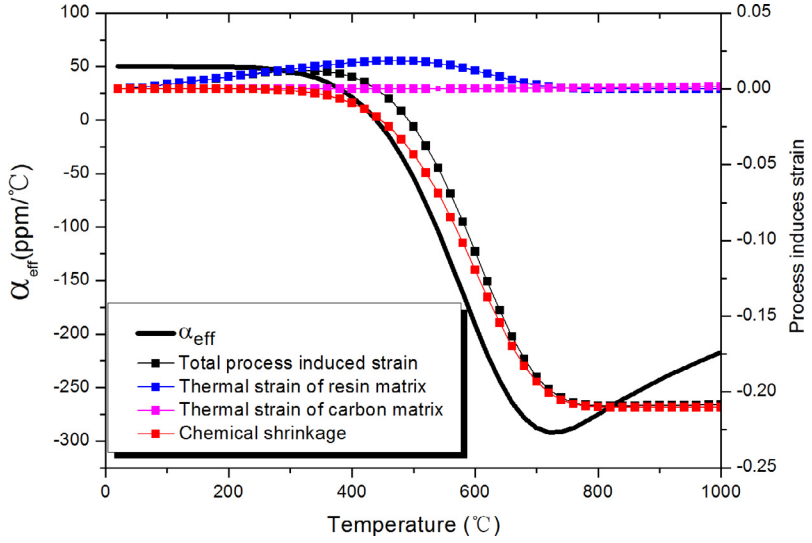

Fig. 4. Thermal strain and the apparent thermal expansion coefficient.

responding damage distribution is presented in Fig. 6. When T = 300 °C, as can be seen in Fig. 5(a), $\sigma_{\theta\theta}$ is mainly compressive stress and the larger $\sigma_{\theta\theta}$ appears both at region along the interface and around point 'A'. Here, as pyrolysis reaction does not start, matrix expands with 50 (ppm/°C). The fiber acts as a constraint to prevent the matrix expanding which results in significant compressive stress at these regions. Fig. 5(b) shows the stress distribution at T = 487 °C. The stress pattern is similar to the one at T = 300 °C, but the stress sign has changed to opposite. Because the chemical shrinkage starts to dominant the thermal deformation in the carbonization process, the matrix turns to sustain the tensile stress along the fiber/matrix interface. In order to understand the stress development during the process, the evolutions of $\sigma_{\theta\theta}$ at points of 'A', 'B' and 'C' are plotted in Fig. 7. At first, before activation of the pyrolysis reaction, the circumferential stress in the matrix is in compression status due to thermal expansion mismatch of fibers and resin and the magnitude increases with temperature. Then, as the description in Fig. 4, from the thermal pyrolysis initiation at T = 300 °C, the chemical shrinkage of matrix gradually play the leading role in the thermal deformation, as a result, the stress drops down. And $\sigma_{\theta\theta}$ changes to be zero when the apparent thermal expansion coefficient of matrix reaches the value of CTE of fibers (13 ppm/°C). After that, with the apparent thermal expansion coefficient decreasing, $\sigma_{\theta\theta}$ turns to be tension and then keeps increasing until the damage initialization at T = 487 °C.

The evolution of ε_{max} is also plotted in Fig. 7. When T = 487 °C, ε_{max} firstly reaches the damage initialization criterion at 'A', and damage appears accompanied by matrix softening and stress redistribution. Therefore, as Figs. 7 and 8 shows, the stress at 'A' drops and the strain increases more steeply. Shortly after the damage initializes at 'A', as Fig. 6(c) (T = 500 °C) demonstrated, the damage starts to extend towards the interface. Therefore the stress at region 'B' falls off, and then the location of larger $\sigma_{\theta\theta}$ shifts to regions at 45° of interface (around point 'C'). After that, as Fig. 6 (d) (T = 674 °C) shows, damage evolves along the interface toward position of 45°and the magnitude of damage increases. As a result, the stress at region 'C' drops and the strain slope increases as well.

When the magnitude of damage increases to reach one, the material will be completely damaged and crack will appear. To fur-

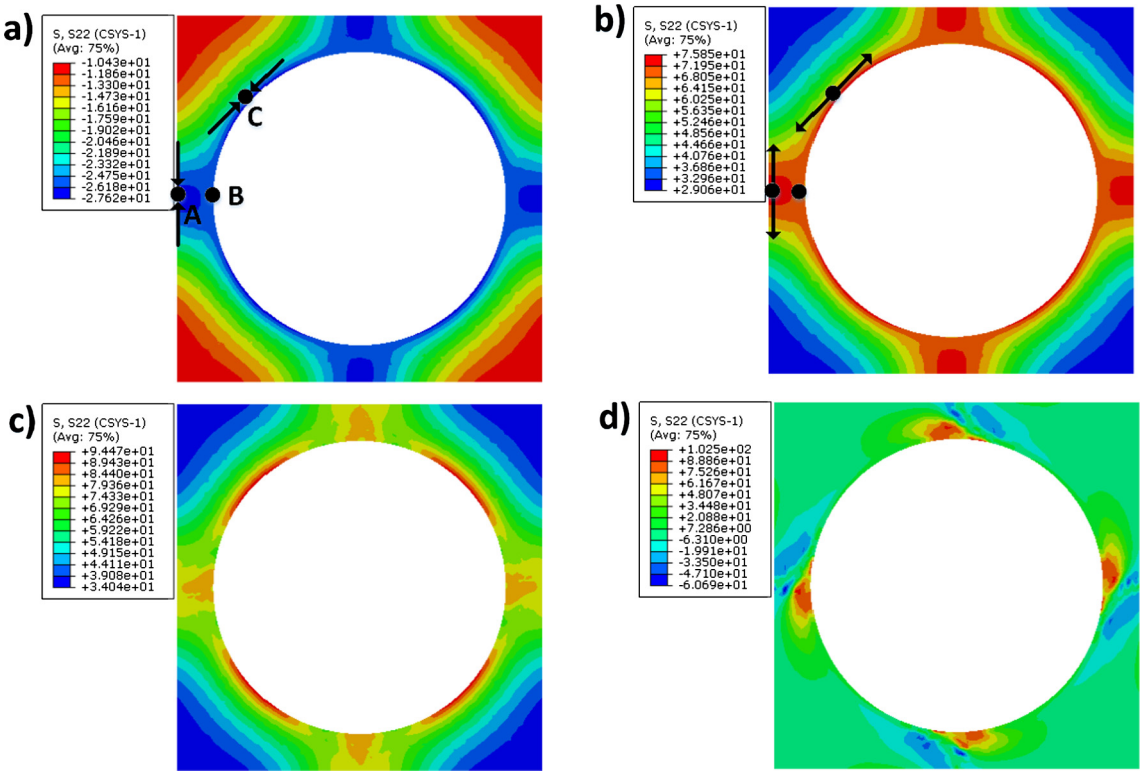

Fig. 5. $\sigma_{\theta\theta}$ at temperature of (a) T = 300 °C, (b) T = 487 °C, (c) T = 500 °C and (d) T = 674 °C.

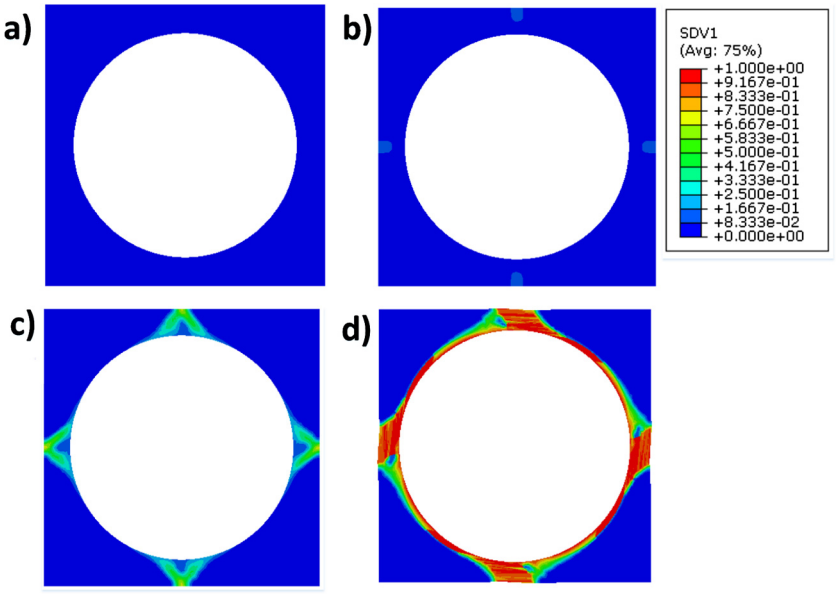

Fig. 6. Damage distribution at temperature of (a) T = 300 °C, (b) T = 487 °C, (c) T = 500 °C and (d) T = 674 °C.

ther understand the pattern and location of crack that may occur, the circumferential, radial, shear and the maximum principal stress along the interface path extrapolated from matrix elements at T = 487 °C are shown in Fig. 9. It can be seen, besides the tensile circumferential stress, the matrix material endures compressive radial stress and interfacial shear stress. Because the magnitude of the radial and shear stresses are much lower than circumferential stress, $\sigma_{\theta\theta}$ is the major one to cause damage. With the pyrolysis progress, the matrix shrinkage is aggravated and thus leads to accumulation of damage. As a result, micro cracks may emerge along the fiber and matrix interface. The similar micro cracks pattern has been reported in the literature [27].

5. Conclusions

In the present work, a meso-mechanical model is established to study the stress and damage development during the carbonization process for carbon/carbon composites manufacture. The evolution of phase volume fractions, mechanical properties and

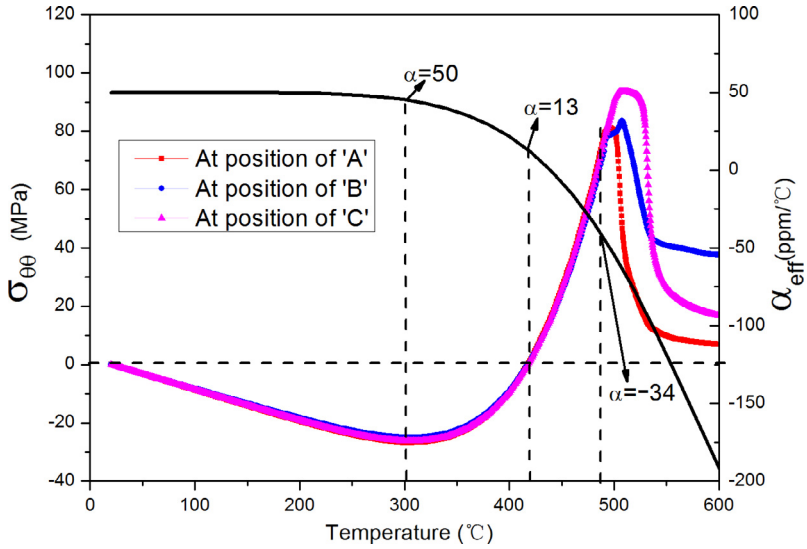

Fig. 7. The development of $\sigma_{\theta\theta}$ at positions of 'A', 'B' and 'C'.

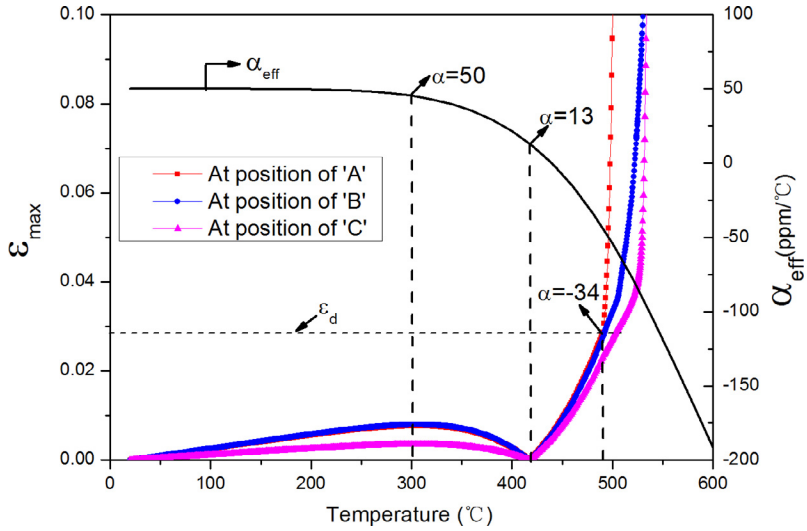

Fig. 8. The development of ε_{max} at positions of 'A', 'B' and 'C'.

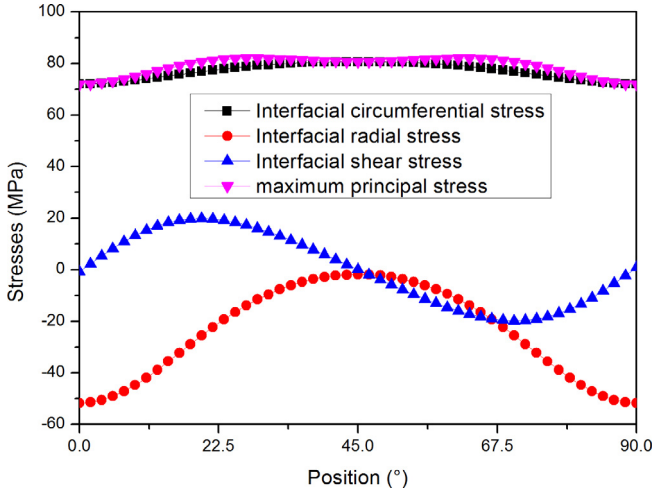

Fig. 9. The stress components and the maximum principle stress along the interface path at T = 487 °C.

thermal deformation are analyzed during the carbonization process. Pyrolysis reaction starts when the temperature reaches 300 °C, and after that, the volume fraction of resin reduces from 100% to zero, with the volume fraction of carbon and voids increasing from 0 to 58% and 42% during the whole process. With the variation of phase fraction volume, the effective elastic modulus of matrix declines at the initial stage of the reaction due to the appearance of voids, and then turns to increase due to the increased carbon which has much higher elastic modulus. Finally, the effective elastic modulus of matrix would reaches about 4.11 GPa. The thermal deformation behaviors of matrix show two different stages with the temperature increasing. The first stage is before the pyrolysis reaction start, in which the thermal deformation is mainly comes from the thermal expansion of resin. The second stage initiates as the chemical decomposition begin and the chemical shrinkage domains the thermal deformation of matrix, which leads the negative strain of matrix. And with the FE model, the internal stress evolution and damage development of the RVE are studied. With the pyrolysis reaction activating, the circumferential stress in the matrix gradually changes from com-

pression status to tension status, which is caused by the different stage of thermal deformation behaviors. When temperature reaches 487 °C, the damage initiate at the point 'A' due to the tensile circumferential stress. With the damage initiation, the local elastic properties vary and the internal stress is redistributed. The damage develops along the fiber/matrix interface with the temperature increasing. With the accumulation of damage, the potential micro crack may emerge along the fiber/matrix interface, which is similar as the literature reported.

Acknowledgments

Financial supports from the National Natural Science Foundation of China (Grant No. 11372301), the Fundamental Research Funds for the Central Universities (WK2480000002), and the Strategic Priority Research Program of the Chinese Academy of Sciences (Grant No. XDB22040502) are gratefully acknowledged. This work is also supported by Collaborative Innovation Center of Suzhou Nano Science and Technology.

References

[1] J. Lachaud, G.L. Vignoles, A Brownian motion technique to simulate gasification and its application to C/C composite ablation, Comp. Mater. Sci. 44 (4) (2009) 1034–1041.
[2] Y. Xu, W. Zhang, D. Chamoret, M. Domaszewski, Minimizing thermal residual stresses in C/SiC functionally graded material coating of C/C composites by using particle swarm optimization algorithm, Comp. Mater. Sci. 61 (2012) 99–105.
[3] T. Yin, Z. Zhang, X. Li, X. Feng, Z. Feng, Y. Wang, et al., Modeling ablative behavior and thermal response of carbon/carbon composites, Comp. Mater. Sci. 95 (2014) 35–40.
[4] J.D. Nam, J.C. Seferis, Composite methodology for multistage degradation of polymers, J. Polym. Sci., Part B: Polym. Phys. 29 (5) (1991) 601–608.
[5] J.D. Nam, J.C. Seferis, Generalized composite degradation kinetics for polymeric systems under isothermal and nonisothermal conditions, J. Polym. Sci., Part B: Polym. Phys. 30 (5) (1992) 455–463.
[6] J.D. Nam, J.C. Seferis, Initial polymer degradation as a process in the manufacture of carbon-carbon composites, Carbon 30 (5) (1992) 751–761.
[7] Y. Dimitrienko, Modelling of the mechanical properties of composite materials at high temperatures: Part 1 Matrix and fibers, Appl. Compos. Mater. 4 (4) (1997) 219–237.
[8] Y. Dimitrienko, Modelling of the mechanical properties of composite materials at high temperatures: Part 2. Properties of unidirectional composites, Appl. Compos. Mater. 4 (4) (1997) 239–261.
[9] Y. Dimitrienko, Modelling of the mechanical properties of composite materials at high temperatures. Part 3. Textile composites, Appl. Compos. Mater. 5 (4) (1998) 257–272.
[10] Y.I. Dimitrienko, Mechanics of porous media with phase transformations and periodical structures 1. Method of asymptotic averaging, Eur. J. Mech.-A/Solids 17(2) (1998) 305–19.
[11] Y.I. Dimitrienko, Mechanics of porous media with phase transformations and periodical structures 2. Solutions of local and global problems, Eur. J. Mech.-A/Solids 17(2) (1998) 321–37.
[12] F.K. Wittel, J. Schulte-Fischedick, F. Kun, B.-H. Kröplin, M. Frieß, Discrete element simulation of transverse cracking during the pyrolysis of carbon fibre reinforced plastics to carbon/carbon composites, Comp. Mater. Sci. 28 (1) (2003) 1–15.
[13] J. Schulte Fischedick, A. Zern, J. Mayer, M. Ruehle, H. Voggenreiter, The crack evolution on the atomistic scale during the pyrolysis of carbon fibre reinforced plastics to carbon/carbon composites, Compos. Part A: Appl. Sci. Manuf. 38 (10) (2007) 2237–2244.
[14] J. Schulte Fischedick, S. Seiz, N. Lützenburger, A. Wanner, H. Voggenreiter, The crack development on the micro- and mesoscopic scale during the pyrolysis of carbon fibre reinforced plastics to carbon/carbon composites, Compos. Part A: Appl. Sci. Manuf.. 38 (10) (2007) 2171–2181.
[15] J. Schulte Fischedick, M. Frieß, W. Krenkel, R. Kochendörfer, M. König, Crack microstructure during the carbonization of carbon fibre reinforced plastics to carbon/carbon composites, in: Proceedings of the 12th Int Conference on Composite Materials (ICCM-12), 1999, pp. 5–7.
[16] J. Kima, W.I. Leea, S.W. Tsai, Modeling of mechanical property degradation by short-term aging at high temperatures, Compos. Part B: Eng. 33 (2002) 531–543.
[17] J. Kim, W.I. Lee, K. Lafdi, Numerical modeling of the carbonization process in the manufacture of carbon/carbon composites, Carbon 41 (13) (2003) 2625–2634.
[18] J. Kim, K. Lafdi, W.I. Lee, Numerical simulation of the carbonization process in the manufacturing of carbon–carbon composites. I. Material characterization, in: 24th Biennial Conference on Carbon, Charleston (USA), 1999, pp. 134–5.
[19] J. Kim, K. Lafdi, W.I. Lee, Numerical simulation of the carbonization process in the manufacturing of carbon-carbon composites: II. Numerical analysis, in: 24th Biennial Conference on Carbon, Charleston (USA), 1999, pp. 136–7.
[20] T. Bogetti, J. Gillespie, Process-induced stress and deformation in thick-section thermoset composite laminates, J. Compos. Mater. 26 (5) (1992) 626–660.
[21] R. Sharma, P. Mahajan, R.K. Mittal Image based finite element analysis of 3D-orthogonal carbon-carbon (C/C) composite, in: Proceedings of the World Congress on Engineering 2010 Vol II WCE 2010, June 30 - July 2, 2010, London, UK, 2010.
[22] R. Sharma, A.R. Bhagat, P. Mahajan, Finite element analysis for mechanical characterization of 4D inplane carbon/carbon composite with imperfect microstructure, Latin Am. J. Solids Struct. 11 (2014) 170–184.
[23] A. Alghamdi, A. Khan, P. Mummery, M. Sheikh, The characterisation and modelling of manufacturing porosity of a 2-D carbon/carbon composite, J Compos Mater. 48 (23) (2013) 2815–2829.
[24] ABAQUS 6.13 User's Manual. ABAQUS Inc, Pawtucket, RI, USA, 2013.
[25] A. Shigang, F. Daining, H. Rujie, P. Yongmao, Effect of manufacturing defects on mechanical properties and failure features of 3D orthogonal woven C/C composites, Composites Part B 71 (2015) 113–121.
[26] C. Heinrich, M. Aldridge, A.S. Wineman, J. Kieffer, A.M. Waas, K.W. Shahwan, The role of curing stresses in subsequent response, damage and failure of textile polymer composites, J. Mech. Phys. Solids 61 (5) (2013) 1241–1264.
[27] E. Fitzer, L.M. Manocha, Microstructure of carbon/carbon composites, Springer, Berlin Heidelberg, 1998.